SUPPLEMENTARY MATERIAL

Fig. S1. The expression of Notch targets is suppressed in endocycling follicle cells where E(y)1 function is compromised. (A,A') Induction of an independent *e(y)1*-RNAi transgene suppressed *hnt* expression in the *e(y)1*-RNAi follicle cells of a stage-7 egg chamber, marked by the expression of RFP (red, A). (B,B') Expression of *brE-lacZ* was abolished in mid-stage follicle cells with *e(y)1* depleted [expressing GFP (red, B)].

Fig. S2. The M/E switch is disrupted in the *e(y)1*-RNAi follicle cells. (A,A') The nuclei of *e(y)1*-depeleted follicle cells (expressing RFP) in a stage-8 egg chamber are much smaller and more crowded than those of their neighboring wild-type cells (lacking RFP). (B,B') In an egg chamber at stage 8, PH3 was detected in the *e(y)1*-knockdown follicle cells (expressing RFP), but not in wild-type cells (lacking RFP). (C,C') After stage 7, CycB, which is normally suppressed in wild-type endocycling follicle cells (lacking RFP), was randomly expressed in the *e(y)1*-RNAi follicle cell clones (expressing RFP). Cell nuclei were co-stained with DAPI (green in A' and blue in B,C).

Fig. S3. Poor viability of *e(y)1* mutant cells in the wing disc and Lateral inhibition defects in *e(y)1*-depeleted tissues. (A-A'') Wild-type *FRT19A* mock clones in a wing disc. (B-B'') The sizes of *e(y)1* mutant clones generated in a *Minute*$^{+/-}$ [*M(1)*$^{osp/+}$] background, marked by the absence of GFP, are extremely small, compared with those of control clones in (A-A''). Mosaic clones were induced by heat-shocking early second instar larvae at 37℃ for 1 hour, and wing discs were dissected after 72 hours at 25℃. Cell nuclei were labeled with DAPI in red (A'', B''). (C) An adult scutellum bearing *FRT19A* mock clones had four well-organized bristles (white arrows). (D) A fly with *e(y)1* mutant clones carried an extra bristle in scutellum (yellow arrow, in 8 out of 50 adult flies observed). (E) Portion of an adult wing with *FRT19A* mock clones. (F) Extra vein-like structures (black arrows) observed in an adult wing carrying *e(y)1* mutant clones. (G) Portion of a *C96-Gal4* control wing. (H) Dense wing margin bristles (black arrows) in *C96-Gal4>e(y)1*-RNAi flies .

Fig. S4. Notch gain-of-function phenotypes in Su(H)-VP16-expressing tissues. (A-B') *en-Gal4, UAS-RFP/+; tub-Gal80ts/+* control discs showed normal expression patterns of Notch targets, Cut (A') and Wg (B'). (C-D') Ectopic expression of *Su(H)-VP16* by *en-Gal4* caused wing disc overgrowth and Notch signaling activation, as monitored by expression of Cut (C') and Wg (D') in the posterior compartment of wing discs. (E-H) Although the *C96-Gal4>Su(H)-VP16* adult wing did not show obvious overgrowth (F), when compared with the *C96-Gal4* control (E), it displayed partial loss of wing margin bristles (H, red arrows), a typical Notch gain-of-function phenotype.

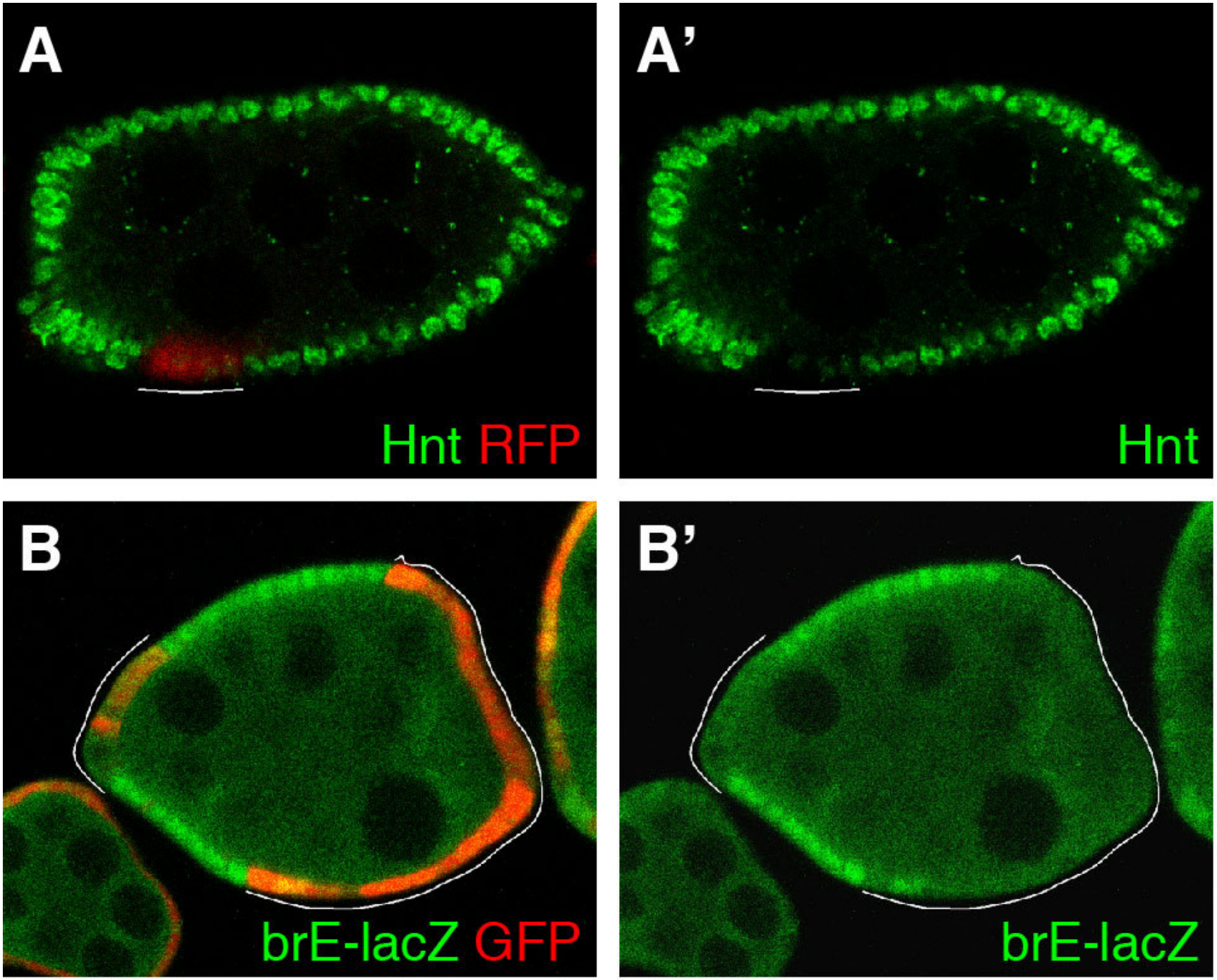

Fig. S1

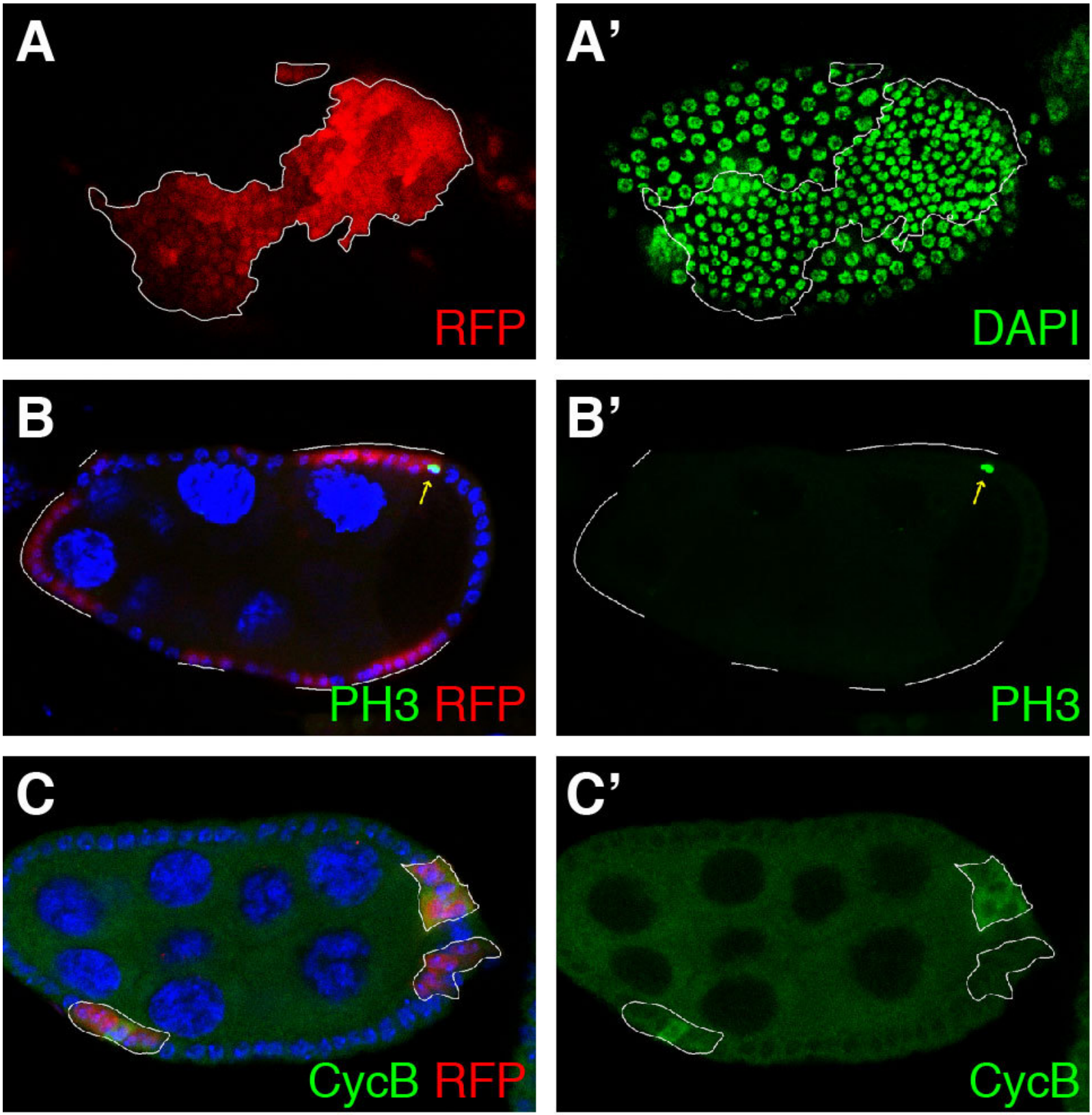

Fig. S2

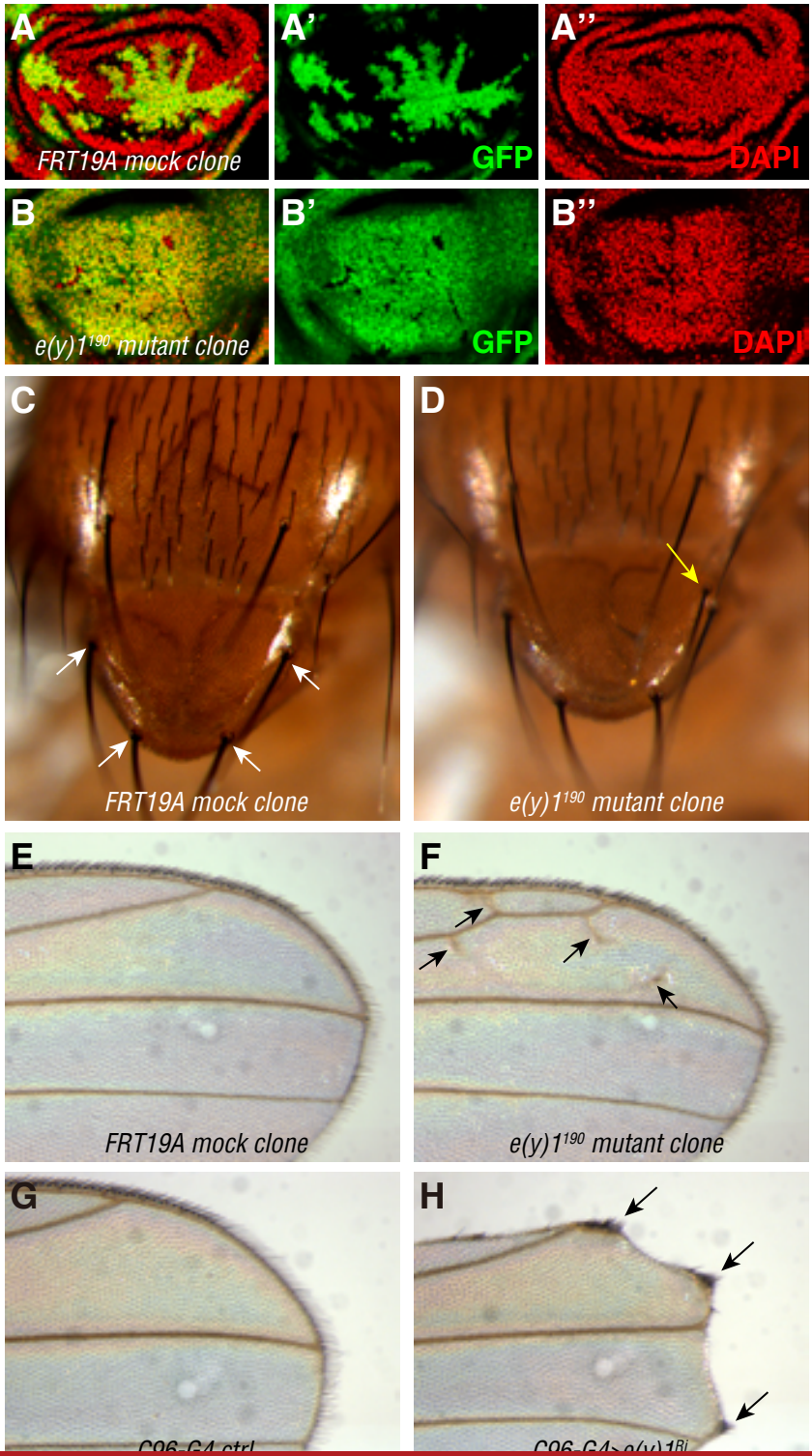
A
FRT19A mock clone
A'
GFP
A''
DAPI
B
e(y)1190 mutant clone
B'
GFP
B''
DAPI
C
FRT19A mock clone
D
e(y)1190 mutant clone
E
FRT19A mock clone
F
e(y)1190 mutant clone
G
C96-G4 ctrl
H
C96-G4> e(y)1Bi

Fig. S3

en-G4, UAS-RFP/+; tub-G80ts/+

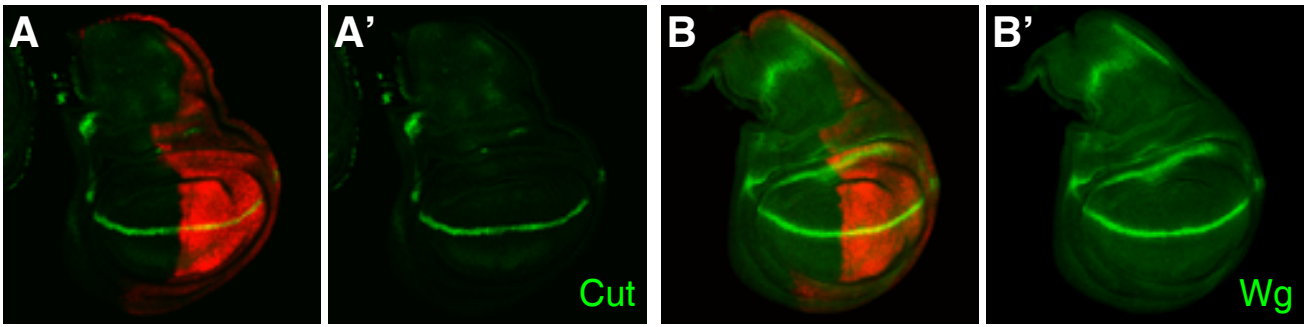

en-G4, UAS-RFP/UAS-Su(H)-VP16; tub-G80ts/+

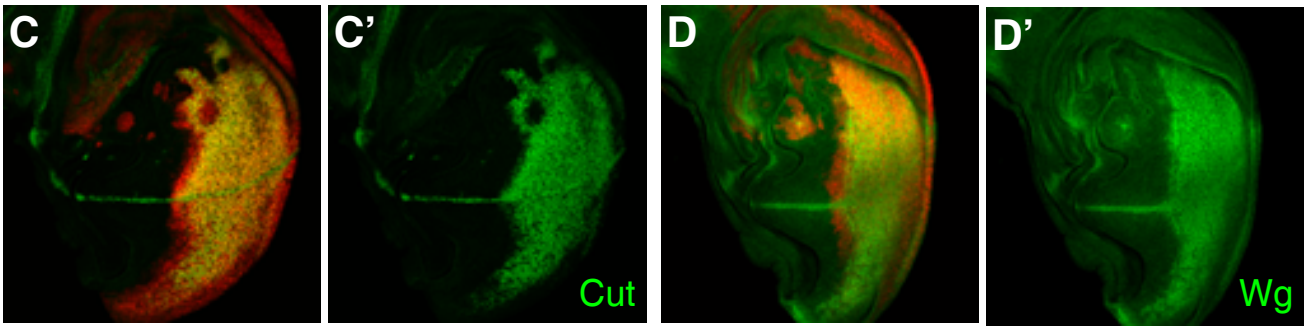

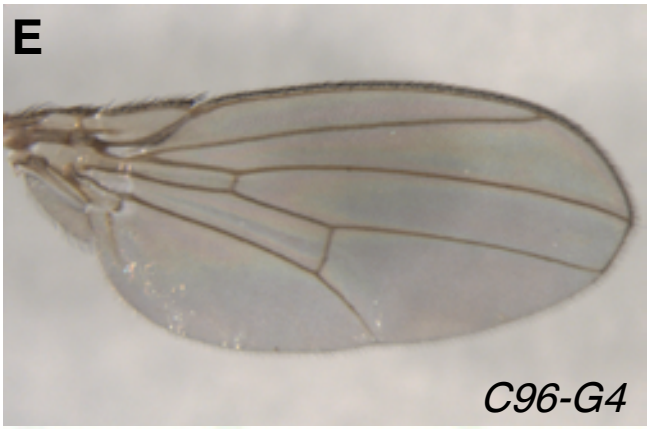

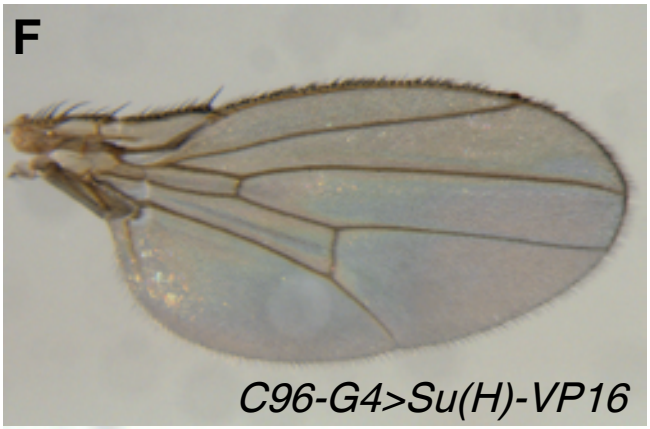

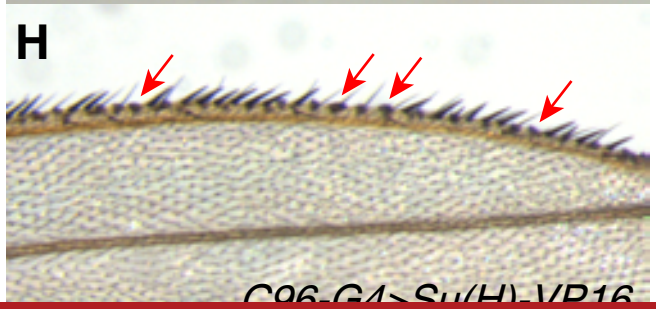

Fig. S4

Table S1: Genotypes related to figures

Figure name	Genotype
Fig. 1A-B’	*hsFLP/+;; act>CD2>Gal4, UAS-RFP/UAS-e(y)1*$^{RNAi\text{-}BL32345}$ (> = FRT in this and all following figures)
Fig. 1C,C’	*hsFLP/+;E(spl)mβ-CD2/+; act>y*$^{+}$*>Gal4, UAS-lacZ/UAS-e(y)1*$^{RNAi\text{-}BL32345}$
Fig. 1D,D’	*hsFLP/+; act>y*$^{+}$*>Gal4, UAS-GFP/+; E(spl)m7-lacZ/UAS-e(y)1*$^{RNAi\text{-}BL32345}$
Fig. 2B-C’’	*ubi-mRFPnls, w, hsFLP*^{122} *FRT19A/w, hsFLP*^{122} *e(y)1*^{190} *FRT19A*
Fig. 2D	*w, ubi-GFP,M(1)*^{osp} *FRT19A/w, hsFLP*^{122} *e(y)1*^{190} *FRT19A;; +/TM6B*
Fig. 2E	*w, ubi-GFP,M(1)*^{osp} *FRT19A/w, hsFLP*^{122} *e(y)1*^{190} *FRT19A;; Dp(1;3)DC335/+*
Fig. 3A	*w*^{1118}
Fig. 3B	*C96-Gal4/UAS-e(y)1*$^{RNAi\text{-}BL32345}$
Fig. 3C	*N*$^{264\text{-}39}$*/+*
Fig. 3D	*N*$^{264\text{-}39}$*/+;;* C96-*Gal4/UAS-e(y)1*$^{RNAi\text{-}BL32345}$
Fig. 3E	*N*$^{264\text{-}39}$*/P{GT1}e(y)1*^{BG00948}
Fig. 3F	*N*$^{264\text{-}39}$*/e(y)1*^{190}
Fig. 3G	*N*^{1}*/+*
Fig. 3H	*N*^{1}*/e(y)1*^{190}
Fig. 3I,J	*en-Gal4, UAS-GFP/+; tub-Gal80ts/+*
Fig. 3K,L	*en-Gal4, UAS-GFP/+; tub-Gal80ts/UAS-e(y)1*$^{RNAi\text{-}BL32345}$
Fig. 4A,A’	*hsFLP/+;; act>CD2>Gal4, UAS-RFP/UAS-e(y)1*$^{RNAi\text{-}BL32345}$
Fig. 4B,B’	*hsFLP/+; UAS-N*^{EXT}*/+; act>CD2>Gal4, UAS-RFP/UAS-e(y)1*$^{RNAi\text{-}BL32345}$
Fig. 4C,C’	*hsFLP/+; UAS-N*^{ICD}*/+; act>CD2>Gal4, UAS-RFP/UAS-e(y)1*$^{RNAi\text{-}BL32345}$
Fig. 4D,D’	*hsFLP/+; UAS-Su(H)-VP16/+; act>CD2>Gal4, UAS-RFP/UAS-e(y)1*$^{RNAi\text{-}BL32345}$
Fig. 4E	*C96-Gal4/+*
Fig. 4F	*C96-Gal4/UAS-e(y)1*$^{RNAi\text{-}BL32345}$
Fig. 4G	*UAS-N*^{ICD}*/+; C96-Gal4/UAS-e(y)1*$^{RNAi\text{-}BL32345}$
Fig. 4H	*UAS-Su(H)-VP16/+; C96-Gal4/UAS-e(y)1*$^{RNAi\text{-}BL32345}$
Fig. 6A	*en-Gal4, UAS-GFP/+; tub-Gal80ts/UAS-TAF12*$^{RNAi\text{-}BL34852}$
Fig. 6B	*en-Gal4, UAS-GFP/+; tub-Gal80ts/UAS-TAF1*$^{RNAi\text{-}BL32421}$
Fig. 6C	*en-Gal4, UAS-GFP/UAS-e(y)2*$^{RNAi\text{-}BL42524}$*; tub-Gal80ts/+*
Fig. 6D	*C96-Gal4/UAS-TAF12*$^{RNAi\text{-}BL34852}$
Fig. 6E	*C96-Gal4/UAS- UAS-TAF1*$^{RNAi\text{-}BL32421}$
Fig. 6F	*UAS-e(y)2*$^{RNAi\text{-}BL42524}$*/+; C96-Gal4/+*
Fig. S1A,A’	*hsFLP/+; UAS-e(y)1*$^{NIG\text{-}6474R\text{-}1}$*/+; act>CD2>Gal4, UAS-RFP/UAS-dcr2*

Fig. S1B,B'	*hsFLP/+; act>y^{+}>Gal4, UAS-GFP/+; br-lacZ/UAS-e(y)1$^{RNAi\text{-}BL32345}$*
Fig. S2A-C'	*hsFLP/+;; act>CD2>Gal4, UAS-RFP/UAS-e(y)1$^{RNAi\text{-}BL32345}$*
Fig. S3A-A''	*w, ubi-GFP,M(1)^{osp} FRT19A/w, hsFLP^{122} FRT19A*
Fig. S3 B-B''	*w, ubi-GFP,M(1)^{osp} FRT19A/w, hsFLP^{122} e(y)1^{190} FRT19A*
Fig. S3C	*ubi-mRFPnls, w, hsFLP^{122} FRT19A/w, hsFLP^{122} FRT19A*
Fig. S3D	*ubi-mRFPnls, w, hsFLP^{122} FRT19A/w, hsFLP^{122} e(y)1^{190} FRT19A*
Fig. S3E	*w, ubi-GFP,M(1)^{osp} FRT19A/w, hsFLP^{122} FRT19A*
Fig. S3F	*w, ubi-GFP,M(1)^{osp} FRT19A/ w, hsFLP^{122} e(y)1^{190} FRT19A*
Fig. S3G	*C96-Gal4/+*
Fig. S3H	*C96-Gal4/UAS-e(y)1$^{RNAi\text{-}BL32345}$*
Fig. S4A-B'	*en-Gal4, UAS-RFP/+; tub-Gal80ts/+*
Fig. S4C-D'	*en-Gal4, UAS-RFP/UAS-Su(H)-VP16; tub-Gal80ts/+*
Fig. S4E,G	*C96-Gal4/+*
Fig. S4F,H	*UAS-Su(H)-VP16/+; C96-Gal4/+*